European Journal of Medicinal Chemistry 45 (2010) 2957–2971

Contents lists available at ScienceDirect

European Journal of Medicinal Chemistry

journal homepage: http://www.elsevier.com/locate/ejmech

Original article

Functionalized aurones as inducers of NAD(P)H:quinone oxidoreductase 1 that activate AhR/XRE and Nrf2/ARE signaling pathways: Synthesis, evaluation and SAR

Chong-Yew Lee, Eng-Hui Chew, Mei-Lin Go*

Department of Pharmacy, National University of Singapore, 18 Science Drive 4, Singapore 117543, Singapore

ARTICLE INFO

Article history:
Received 18 December 2009
Received in revised form
15 March 2010
Accepted 16 March 2010
Available online 25 March 2010

Keywords:
Aurones
Chemoprevention
NAD(P)H:quinone oxidoreductase 1
Phase II enzyme inducers

ABSTRACT

The chemopreventive potential of functionalized aurones and related compounds as inducers of NAD(P)H:quinone oxidoreductase 1 (NQO1, EC 1.6.99.2) are described. Several 4,6-dimethoxy and 5-hydroxyaurones induced NQO1 activity of Hepa1c1c7 cells by 2-fold at submicromolar concentrations, making these the most potent inducers to be identified from this class. Mechanistically, induction of NQO1 was mediated by the activation of AhR/XRE and Nrf2/ARE pathways, indicating that aurones may be mixed activators of NQO1 induction or agents capable of exploiting the proposed cross-talk between the AhR and Nrf2 gene batteries. QSAR analysis by partial least squares projection to latent structures (PLS) identified size parameters, in particular those associated with non-polar surface areas, as an important determinant of induction activity. These were largely determined by the substitution on rings A and B. A stereoelectronic role for the exocyclic double bond as reflected in the E_{LUMO} term was also identified. The electrophilicity of the double bond or its effect on the conformation of the target compound are possible key features for induction activity.

1. Introduction

Cancer chemoprevention is a strategy aimed at reducing the risk of cancer by avoiding exposure to cancer-causing agents, enhancing host defense mechanisms, lifestyle adjustments and supplementation with chemopreventive agents that inhibit, reverse or block tumorigenesis [1–3]. Many chemopreventive agents are dietary phytochemicals such as sulforaphane from broccoli, glucosinolate-derived indoles found in cruciferous vegetables and structurally diverse flavonoids that are present in fruits, vegetables and plant-derived beverages [4–6]. These bioactive compounds selectively modulate the expression levels or biological activities of key proteins involved in various cell signaling cascades, particularly enzymes involved in the detoxification of xenobiotics [7–10]. The enzyme NAD(P)H:quinone oxidoreductase 1 (NQO1, EC 1.6.99.2) has received particular attention in this regard because the induction of NQO1 provides the cell with multiple layers of protection against environmental insults [8]. Briefly, NQO1 detoxifies highly reactive quinones to quinols without generating reactive semiquinones and maintains endogenous lipid soluble antioxidants in their reduced and active forms. It has also been reported to stabilize the tumor suppressor p53 in response to DNA-damaging stimuli [11]. The induction of NQO1 in vivo and in vitro is correlated to the induction of other protective phase II enzymes and this has led to its reputation as a reasonable biomarker for evaluating the chemopreventive potential of target compounds [12].

Aurones (2-benzylidenebenzofuran-3(*2H*)-ones) are a class of flavonoids found in fruits and flowers where they function as phytoalexins against infections and contribute to the yellow pigmentation of plant parts [13]. Our interest in aurones centers on their potential to enhance NQO1 activity and hence function as chemopreventive agents. Jang and co-workers have reported two aurones (sulfuretin and 6,4′-dihydroxy-3′-methoxyaurone, Fig. 1) isolated from the seeds of the Tonka Bean (*Dipteryx odorata*) that induced NQO1 activity in murine hepatoma cells [14]. Structurally, aurones possess features that are associated with NQO1 induction activity, the most prominent of which is the presence of a Michael acceptor moiety. In addition, the olefinic double bond of this moiety is exocyclic in aurones. Talalay et al. noted greater NQO1 induction potencies among Michael acceptors with exocyclic double bonds (for example, 2-methylene-4-butyrolactone and 3-methylene-2-norbornanone) as compared to others such as furan-2(*5H*)-one where the double bond is endocyclic [15]. They proposed that the exocyclic location of the double bond enhanced the electrophilic reactivity of the Michael acceptor moiety, resulting in greater NQO1 induction activity. If this motif is indeed associated with greater

* Corresponding author. Tel.: +65 65162654; fax: +65 67791554.
E-mail address: phagoml@nus.edu.sg (M.-L. Go).

0223-5234/$ – see front matter © 2010 Elsevier Masson SAS. All rights reserved.
doi:10.1016/j.ejmech.2010.03.023

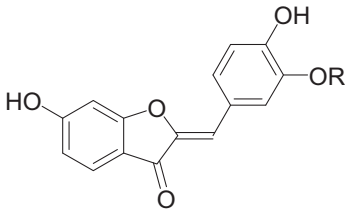

Fig. 1. Structures of sulfuretin (R = H) and 6,4′-dihydroxy-3′-methoxyaurone (R = CH_3).

reactivity, then aurones which are unique among flavonoids in having an exocyclic double bond, should be outstanding inducers. On the other hand, only modest induction potencies were found for sulfuretin and 6,4′-dihydroxy-3′-methoxyaurone [14]. It may be argued that the NQO1 induction potential of aurones has not been fully exploited and that structural modifications of the scaffold would result in more potent members.

The mechanism of NQO1 induction by aurones is also of interest. In a previous study, flavonoids were classified as bifunctional inducers because they induced both Phase I and Phase II metabolic enzymes by a mechanism that involves activation of the aryl hydrocarbon receptor (AhR)-xenobiotic-response element (XRE) pathway [15,16]. Briefly, the flavonoid binds to cytosolic AhR leading to its translocation to the nucleus where it causes transcriptional activation of Phase I enzymes like cytochrome P450-1A1 (CYP1A1) and Phase II enzymes (NQO1, glutathione S-transferase among others) [10,17,18]. Phase II enzymes play a key role in detoxification whereas Phase I enzymes (CYP1A1) activate polycyclic aromatic hydrocarbons to ultimate carcinogens [19]. Thus inducers that affect both Phase I and II enzymes are generally considered to be less promising chemopreventive agents compared to monofunctional inducers that selectively activate Phase II enzymes [20]. Mechanistically, monofunctional inducers (which are usually electrophiles) interact with cysteine residues in Kelch-like erythroid cell derived protein 1 (Keap1), a binding partner of nuclear factor-erythroid related factor 2 (Nrf2) that is involved in regulating its transcriptional activity by sequestering the cytosolic Nrf2 and targeting it for proteosomal degradation. Consequently, increased accumulation of nuclear Nrf2 accelerates transcription of Phase II enzymes through activation of the antioxidant response element (ARE) of the relevant genes [21]. However, recent findings showed that several flavonoids behave as mixed AhR/Nrf2 activators and induced Phase II enzymes by activating both ARE- and XRE-signaling pathways [10,22]. The few mixed activators identified to date are structurally diverse, such as flavonoids (quercetin, luteolin, chrysin), 1,2-dithiol-3-thiones and oltipraz [10]. It has been argued that by acting on dual signaling pathways, mixed activators bring about a greater chemopreventive effect than mono- or bifunctional inducers [23,24].

In this study, a series of functionalized aurones were investigated for their ability to induce NQO1 in Hepa1c1c7 cells. We showed here that the more potent aurones induced NQO1 by activating both the AhR/XRE and Nrf2/ARE pathways and discussed the structure–activity relationships associated with their NQO1 induction activities.

2. Chemical considerations

2.1. Design of target compounds

Anecdotal evidence suggests that changes in the substitution on ring A of the aurone scaffold have a marked effect on biological activity. Lawrence and co-workers noted that 5,6,7-trimethoxyaurones had greater cell growth inhibitory properties than their corresponding 4,5,6-trimethoxy regioisomers [25]. Investigations on the inhibitory effects of aurones on the tyrosinase enzyme in human melanocytes showed that the most active compounds had hydroxyl groups on ring A as compared with less active compounds that had rings A that were either unsubstituted or had only one hydroxyl group [26]. Based on these observations, we synthesized five series of aurones with different ring A substituents. These are 4,6-dimethoxyaurones (Series 1), 4,6-dihydroxyaurones (Series 2), monohydroxylated aurones (Series 3 and 4) and aurones without substituents on ring A (Series 5). The choice of methoxy and hydroxy groups was based on the prevalence of these groups in naturally occurring aurones [27]. Isomeric isoaurones (Series 6, 7) in which the carbonyl function is embedded as a lactone, unlike the ketone carbonyl in aurones, were also synthesized. Series 8 were dehydroaurones in which the exocyclic double bond is reduced. The structures of compounds in Series 1–8 are given in Table 1. In addition, the substitution pattern on ring B was varied to include groups with different lipophilicity and electron donating/withdrawing properties [28].

Table 1
Structures of compounds in Series 1–8.

Compound	R^1	% Yield	Compound	R^1	% Yield
Series 1	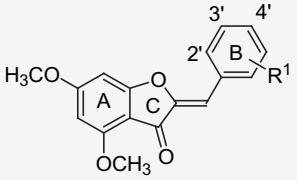				
1-1	H	40	**1-15**	4′-F	80
1-2	2′-Cl	90	**1-16**	4′-CN	67
1-3	3′-Cl	60	**1-17**	4′-CF_3	46
1-4	4′-Cl	46	**1-18**	4′-NO_2	38
1-5	2′-OH	98	**1-19**	2′-CH_3	37
1-6	3′-OH	54	**1-20**	4′-CH_3	65
1-7	4′-OH	43	**1-21**	4′-$N(CH_3)_2$	21
1-8	2′, 3′-$(OH)_2$	15	**1-22**	4′-*N*-methylpiperazinyl	20
1-9	2′, 4′-$(OH)_2$	20	**1-23**	2′-pyridinyl[a]	20
1-10	2′-OCH_3	94	**1-24**	3′-pyridinyl[a]	27
1-11	3′- OCH_3	20	**1-25**	4′-pyridinyl[a]	30
1-12	4′- OCH_3	74	**1-26**	3′-quinolinyl[a]	51
1-13	2′-F	58	**1-27**[b]	4,6-Dimethoxybenzofuran-3(2*H*)-one	56
1-14	3′-F	37			
Series 2	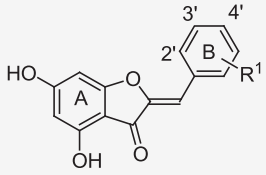				
2-1	H	15	**2-9**	3′-OCH_3	68
2-2	2′-Cl	44	**2-10**	4′-OCH_3	31
2-3	3′-Cl	23	**2-11**	4′-CN	20
2-4	4′-Cl	16	**2-12**	4′-CH_3	65
2-5	2′-OH	31	**2-13**	2′-F	28
2-6	3′-OH	43	**2-14**	3′-OCH_3, 4′-OH	15
2-7	4′-OH	62	**2-15**	3′, 4′, 5′-$(OCH_3)_3$	32
2-8	2′-OCH_3	35	**2-16**[c]	4,6-Dihydroxybenzofuran-3(2*H*)-one	88

Table 1 (*continued*)

Compound	R^1	% Yield	Compound	R^1	% Yield
Series 3					
		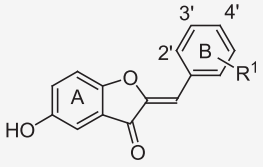			
3-1	H	25	**3-7**	4′-OH	60
3-2	2′-Cl	55	**3-8**	2′-OCH_3	50
3-3	3′-Cl	22	**3-9**	3′- OCH_3	22
3-4	4′-Cl	58	**3-10**	4′- OCH_3	28
3-5	2′-OH	47	**3-11**	4′-CN	50
3-6	3′-OH	60	**3-12**	4′-CH_3	65
Series 4					
		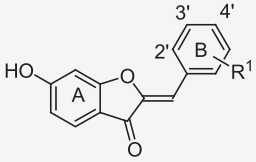			
4-1	H	38	**4-7**	4′-OH	53
4-2	2′-Cl	33	**4-8**	2′-OCH_3	62
4-3	3′-Cl	65	**4-9**	3′- OCH_3	50
4-4	4′-Cl	67	**4-10**	4′- OCH_3	24
4-5	2′-OH	43	**4-11**	4′-CN	76
4-6	3′-OH	30	**4-12**	4′-CH_3	60

Compound	R^1	%Yield
Series 5		
	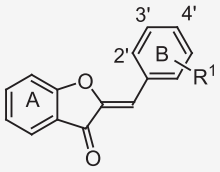	
5-1	2′-OH	65
5-2	2′-Cl	31
Series 6		
	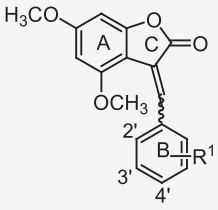	
6-1	H	47
6-2	2′-OH	12
6-3	2′-OCH_3	25
6-4	2′-Cl	48
6-5	4′-Cl	31

Compound	R^1	%Yield	Compound	R^1	%Yield
Series 7					
	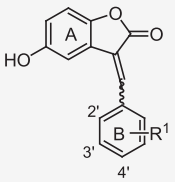				
7-1	H	25	**7-6**	4′-OCH_3	32
7-2	2′-OH	65	**7-7**	2′-Cl	15
7-3	3′-OH	20	**7-8**	4′-Cl	22
7-4	4′-OH	18	**7-9**	2′-F	20
7-5	2′-OCH_3	32	**7-10**	3′-F	31
			7-11	4′-F	55

Compound	R^1	%Yield
Series 8		
	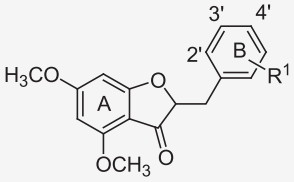	
8-1	H	50
8-2	2′-OH	35

[a] Ring B is replaced by heterocyclic ring.
[b] No R^1 substituent. Benzylidene side chain is omitted.
[c] No R^1 substituent. Benzylidene side chain is omitted.

2.2. Synthetic approaches

87 compounds were synthesized in this investigation, of which 56 have not been previously reported in the SciFinder Scholar™ (Chemical Abstract Service). The synthesis of the 4,6-dimethoxyaurones (Series 1) is shown in Scheme 1. Briefly, 3,5-dimethoxyphenol was reacted with chloroacetic acid in the presence of sodium hydride to give 3,5-dimethoxyphenoxyacetic acid (**1-28**). The acidic side chain was then cyclized by a Friedel-Craft acylation reaction to give the benzofuran-3(*2H*)-one (**1-27**) which reacted with various aldehydes in a base-catalyzed aldol reaction to give the target compounds [25].

In the case of the 4,6-dihydroxyaurones (Series 2), phloroglucinol was reacted with chloroacetonitrile via a Hoesch acylation to give an iminium salt which was hydrolyzed under acidic conditions to give the acetophenone (**2-17**) [26,29]. Base-catalyzed cyclization of **2-17** gave 4,6-dihydroxybenzofuran-3(*2H*)-one (**2-16**) which was condensed with various benzaldehydes by microwave heating (110 °C, 10–15 min) in sealed tubes (Scheme 2). This procedure significantly shortened reaction times and made it unnecessary to protect the phenolic hydroxyl groups prior to aldol condensation. However, **2-13** and **2-14** could not be obtained by this method and their synthesis was achieved by conventional heating and protection of the phenolic hydroxyl groups.

A similar route was followed for the monohydroxylated aurones of Series 3 and 4 (Scheme 3). Starting from either 2′, 5′-dihydroxyacetophenone or 2′, 4′-dihydroxyacetophenone, α-bromination with cupric bromide gave the brominated acetophenones **3-13** and **4-13,** followed by base-catalyzed cyclization to give the hydroxybenzofuran-3(*2H*)-ones (**3-14**, **4-14**) [30]. Aldol condensation with substituted benzaldehydes gave the desired aurones in yields ranging from 22 to 76%.

The 4,6-dimethoxyisoaurones of Series 6 were synthesized by the Kindler-Willgerodt condensation of 3,5-dimethoxy-2-hydroxyacetophenone with morpholine and sulphur to form a thiomorpholide adduct (Scheme 4) [31]. Hydrolysis yielded the corresponding phenylacetic acid (**6-6**) and lactonization of the acid side chain in the presence of phosphorus oxychloride gave the benzofuran-2(*3H*)-one (**6-7**). The latter was reacted with various substituted benzaldehydes in acetic anhydride to give the desired isoaurones.

For Series 5 and 7, straightforward condensation of the commercially available benzofuran-3(2*H*)-one with substituted benzaldehydes under aldol conditions gave the desired products. Series 8

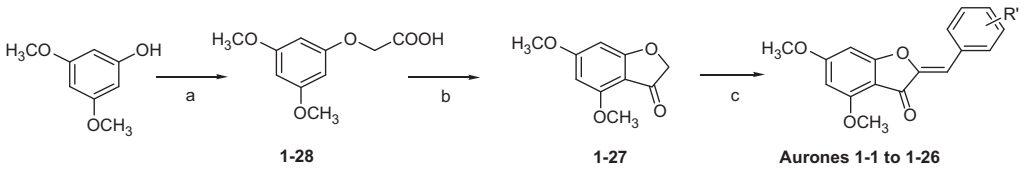

Scheme 1. Reagents and conditions: (a) Chloroacetic acid, NaH, DMF, rt, 12 h. (b) Polyphosphoric acid, 90 °C, 8 h. (c) Substituted benzaldehyde, KOH 50% in water, MeOH, rt, 1–3 h.

comprised of two dehydroaurones which were obtained by hydrogenation of the 4,6-dimethoxyaurones **1-1** and **1-5** in a Parr hydrogenator with palladium on charcoal (10%) as catalyst.

Phenolic hydroxyl groups on reacting benzaldehydes were protected as tetrahydropyranyl ethers which were subsequently removed by acid hydrolysis of the final condensation product. The protection–deprotection step was not necessary for benzaldehydes with *ortho*-hydroxyl groups.

2.3. Stereochemical considerations

The exocyclic double bond in aurones and isoaurones may be *E* (trans) or *Z* (cis). These configurational isomers have characteristic ^{1}H and ^{13}C chemical shifts in the NMR spectra. The chemical shift of the olefinic (β) proton is deshielded in the *E* isomer of aurones and appears downfield (ca 7.01 ppm) compared to the *Z* isomer (ca 6.70 ppm) [29,32]. Both ^{1}H and ^{13}C NMR data of Series 1–5 supported the assignment of *Z*-stereochemistry and this was further confirmed by the x-ray structures of **1-10** and **3-10** which showed the presence of the exocyclic double bond in the thermodynamically more stable *Z* configuration [33,34].

Unlike the aurones, analysis of the NMR spectra of the isoaurones pointed to the presence of a mixture of *E* and *Z* isomers, with the *E* isomer present in larger amounts (80–90%). The chemical shifts of the olefinic CβH and the *ortho*-H atoms attached to ring B were used to distinguish between the *Z* and *E* isomers. The deshielding by the carbonyl group caused the olefinic CβH of *E*-isoaurones to shift downfield by 0.04–0.34 ppm compared with their *Z* counterparts [35]. In addition, a downfield shift (by 0.49–0.77 ppm) was observed for H atoms attached to *ortho* positions (if any) of ring B of *Z*-isoaurones. The predominance of the *E* isomer was established by comparing the integrated areas of the singlet peak assigned to CβH of each isomer.

3. Results

3.1. Induction of NQO1 in Hepa1c1c7 cells

The compounds were screened for induction of NQO1 activity in the murine hepatoma (Hepa1c1c7) cells. Screening was carried out at 5 μM or 25 μM and compounds that increased NQO1 activity by 2-fold or more at either concentration were short-listed for the determination of CD (concentration at which a compound increased NQO1 activity by 2-fold). Results of the initial screen are given in Supplementary Information (Table 1). Three compounds (**1-10**, **1-13**, **1-15**) were screened at 1 μM because they adversely affected cell viability at 5 μM. In all, CD values of 31 compounds and two established NQO1 inducers, sulforaphane (a monofunctional inducer) [36] and β-naphthoflavone (BNF, a bifunctional inducer) [7] were determined (Table 2).

The induction activities of the test compounds revealed some interesting structure–activity trends. An important observation was the inactivity of compounds that did not have an intact olefin. These were the dehydroaurones (**8-1**, **8-2**) in which the double bond was reduced and compounds (**1-27**, **2-16**) where the benzylidene side chain was removed. These findings underscored an important role for the exocyclic double bond and the Michael acceptor moiety of which it is a part for induction activity. Another notable observation is the strong representation of 4,6-dimethoxyaurones (Series 1) among the active compounds in Table 2. Series 1 had the largest number of compounds (8) with submicromolar CD values as well as the most potent inducers (**1-5**, **1-13**, **1-14**) identified in this investigation. Replacement of the methoxy groups with hydroxyl resulted in less potent inducers, as seen from Series 2 to 4. The poor activities of **5-1** and **5-2** clearly signaled the need for maintaining substitution on ring A.

Lactones were reported to be poor NQO1 inducers, possibly due to hydrolytic instability or the weaker electron withdrawing effect of the carbonyl group when it is part of a lactone [15]. As such, the isoaurones were anticipated to be poor inducers and this was duly observed. The isoaurones of Series 6 and 7 were only modest inducers of NQO1 with CD values of 3–25 μM. We did not observe hydrolytic instability of the isoaurones during their syntheses or biological evaluation. Thus the diminished electrophilicity of the exocyclic bond in the isoaurones may be a contributing factor. The 4,6-dimethoxyisoaurones (Series 6) were significantly poorer inducers than their aurone counterparts (Series 1), but the 5-hydroxyisoaurones (Series 7) were comparable to the 5-hydroxyaurones (Series 3). Both Series 3 and 7 were notable in having several potent inducers (CD values 0.47–3.9 μM) which may reflect a special preference for 5-OH on ring A. A few substituents on ring B were consistently associated with good activity across the different Series. These were halogens (in Series 1, 3, 4, 6), hydroxyl (Series 1, 7) and methoxy (Series 1, 6). There was also a preference for the groups to be located at 2′ or 3′ on ring B.

3.2. Induction of NQO1 in mutant murine hepatoma BP^{r}c1 cells

The mutant Hepa1c1c7 cells (BP^{r}c1) contain mutations in the Ah-receptor mediated pathway and do not respond to compounds

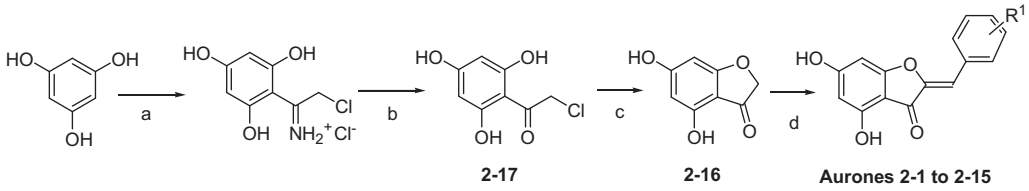

Scheme 2. Reagents and conditions: (a) Chloroacetonitrile, HCl, $ZnCl_2$, Et_2O, 0 °C → rt, 24 h. (b) 1 N HCl, 100 °C, 1 h. (c) NaOAc, MeOH, reflux, 2 h. (d) Substituted benzaldehyde, KOH 50% in water, MeOH, microwave heating, 110 °C, 10–15 min.

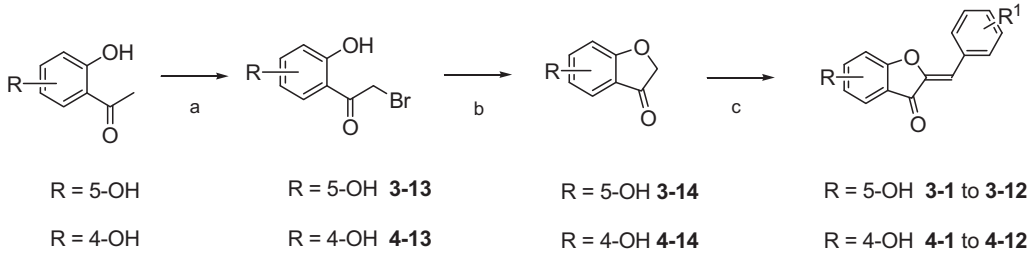

Scheme 3. Reagents and conditions: (a) $CuBr_2$, $CHCl_3$-ethyl acetate, reflux, 8 h. (b) KOH 50%/H_2O, methanol, reflux, 2 h. (c) Substituted benzaldehyde, KOH 50%/H_2O, methanol, 60 °C, 1 h.

that induce NQO1 activity by this route. When investigated on the BP^rc1 cells, none of the compounds in Table 2 induced NQO1 activity which shows that the AhR/XRE signaling pathway was involved in the induction activity of these compounds. Some representative figures are given in Fig. 2. Sulforaphane induced NQO1 activity in the Bp^rc1 cells (CD = 0.34 μM ± 0.01) to almost the same degree as the Hepa1c1c7 cells (CD = 0.21 μM ± 0.02). On the other hand, BNF, like the aurones, did not induce NQO1 activity in Bp^rc1 cells.

3.3. Effect on EROD activity in Hepa1c1c7 cells

To provide further insight on the induction activity of the test compounds, we evaluated their effects on CYP1A1 whose transcription is regulated by the Ah-receptor. CYP1A1 activity in Hepa1c1c7 cells was determined by the ethoxyresorufin-*O*-deethylase (EROD) assay which monitors the formation of fluorescent resorufin when 7-ethoxyresorufin is de-ethylated by CYP1A1. Inducers of CYP1A1 increase resorufin levels and the ratio of its fluorescence in treated versus untreated control cells. The CYP1A1 induction ratios were determined at a fixed concentration (1, 5, 10 or 25 μM) of the test compound (Table 2). Most of the compounds were tested at concentrations that exceeded their CD values for NQO1 induction. As expected, sulforaphane did not induce CYP1A1 activity while BNF, a known bifunctional inducer, showed strong induction activity (ratio of 4.25 at 1 μM). Interestingly, none of the aurones had values of the same magnitude as BNF. Nearly two-third had values that were less than 2, indicating modest induction of CYP1A1 activity even though they were tested at higher concentrations in this assay. These findings raised questions as to whether the aurones only affected the AhR/XRE signaling pathway to bring about NQO1 induction.

3.4. Effect on the Nrf2/ARE signaling pathway

To measure the potential of selected aurones to induce ARE-mediated gene expression, Hepa1c1c7 cells were transiently transfected with a firefly luciferase reporter gene whose expression is regulated by an ARE from the human NQO1 gene (pGL3-ARE) [37]. Compounds that increase NQO1 gene transcription would increase luciferase activity. As seen from Fig. 3, significant increases in luciferase activity were observed for **1-1**, **1-5**, **2-5** and sulforaphane. In contrast, aurones **5-1** and **8-2** which were inactive as NQO1 inducers did not increase luciferase activity. Aurone **2-5** significantly increased luciferase activity only at a higher concentration of 25 μM unlike **1-1** and **1-5** which caused significant increases at both 10 and 25 μM. However, none of the aurones increased luciferase activity to the same degree as sulforaphane, even though some of them (**1-1**, **1-5**) were as active as sulforaphane in inducing NQO1 activity (CD values of 0.2–0.3 μM). The discrepancy between the CD values of the aurones and their effects on the luciferase activities of the transfected cells suggests that while Nrf2/ARE signaling may be essential for NQO1 induction, other pathways may play a more dominant role.

To further probe the involvement of the Nrf2/ARE pathway in the NQO1 induction properties of these aurones, we proceeded to investigate their effects on Nrf2 protein levels. Hepa1c1c7 cells were treated with the test aurone or sulforaphane at 10 μM for 6 h, after which cell lysates were prepared and probed for Nrf2 immunoreactivity (Fig. 4). Densitometric quantitation of the visualized bands of Nrf2 protein revealed by Western analysis showed that only lysates from cells treated with MG132 (a proteosome inhibitor which increases Nrf2 levels), sulforaphane and aurones **1-1**, **1-5**, and **2-5** had significantly higher levels of Nrf2 proteins than control.

The ARE regulatory sequences controlled by Nrf2 are responsible for the transcriptional activation of several genes besides *NQO1*. Here, we probed the effect of the aurones on the functional activity of two proteins whose genes are regulated by the transcriptional activation of ARE consensus sequences by Nrf2. They are γ-glutamylcysteine ligase (GCL) [38] and thioredoxin reductase (TrxR, E.C. 1.8.1.9) [39] GCL is the rate limiting enzyme involved in the de novo synthesis of GSH. Activation of the Nrf2/ARE pathway would bring about up-regulation of GCL and an increase in cellular GSH levels. GSH levels in Hepa1c1c7 cells were determined with Ellman's reagent after incubation (24 h) with selected aurones (10 μM of **1-1**, **1-5**, **2-5**, **5-1**, and **8-2**). As shown in Fig. 5, **1-1**, **1-5** and **2-5** significantly increased GSH content compared to untreated cells but this was not observed for **5-1** and **8-2**.

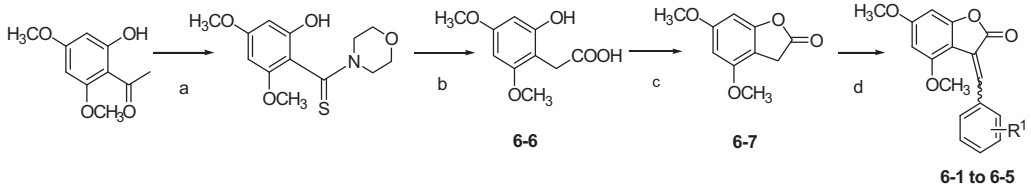

Scheme 4. Reagents and conditions: (a) Sulphur, morpholine, 150 °C, 24 h. (b) 2 M NaOH, reflux, 6 h. (c) $POCl_3$, dichloroethane, rt, 16 h. (d) Substituted benzaldehyde, Et_3N, Ac_2O, 60 °C, 6–12 h.

Table 2
CD values, fold induction of CYP1A1 and E_{LUMO} of test compounds.

Series	Compound	R′ on ring B	CD (μM)[a]	Fold induction of CYP1A1[b]	E_{LUMO} (eV)[c]
Series 1, 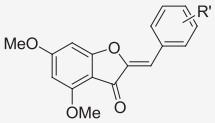	**1-1**	H	0.31 ± 0.02	2.04 ± 0.15 (10 μM)	−1.888
	1-2	2′Cl	0.40 ± 0.07	1.55 ± 0.09 (5 μM)	−2.047
	1-3	3′Cl	0.61 ± 0.05	1.18 ± 0.26 (5 μM)	−2.083
	1-5	2′OH	0.18 ± 0.05	1.87 ± 0.22 (10 μM)	−1.779
	1-6	3′OH	9.8 ± 1.3	1.16 ± 0.05 (25 μM)	−1.876
	1-8	2′, 3′- $(OH)_2$	3.37 ± 0.15	0.97 ± 0.04 (10 μM)	−1.746
	1-10	2′OMe	0.31 ± 0.02	1.56 ± 0.13 (1 μM)	−1.754
	1-13	2′F	0.16 ± 0.10	ND[d]	−1.970
	1-14	3′F	0.15 ± 0.03	1.48 ± 0.02 (5 μM)	−2.025
	1-15	4′F	0.68 ± 0.20	ND[d]	−1.934
	1-23	pyridine-2-yl[e]	3.8 ± 0.5	0.98 ± 0.04 (10 μM)	−2.037
	1-25	pyridine-4-yl[e]	8.5 ± 0.4	1.73 ± 0.23 (25 μM)	−2.228
Series 2, 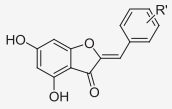	**2-2**	2′Cl	1.7 ± 0.1	1.18 ± 0.11 (10 μM)	−2.135
	2-5	2′OH	3.0 ± 0.26	1.10 ± 0.17 (10 μM)	−1.860
	2-7	4′OH	24.3 ± 1.7	1.05 ± 0.06 (25 μM)	−1.843
	2-9	3′OMe	4.4 ± 0.2	1.13 ± 0.07 (10 μM)	−1.920
	2-13	2′F	5.5 ± 1.1	1.00 ± 0.04 (10 μM)	−2.057
	2-14	3′OMe, 4′OH	16.5 ± 1.2	1.06 ± 0.02 (25 μM)	−1.816
Series 3, 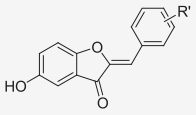	**3-1**	H	3.9 ± 0.4	2.36 ± 0.09 (10 μM)	−2.299
	3-3	3′Cl	0.96 ± 0.17	2.95 ± 0.24 (10 μM)	−2.493
	3-5	2′OH	2.4 ± 0.4	2.01 ± 0.22 (10 μM)	−2.174
	3-8	2′OMe	0.47 ± 0.10	1.68 ± 0.20 (25 μM)	−2.146
Series 4, 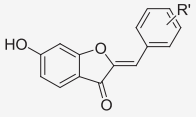	**4-3**	3′Cl	2.8 ± 0.1	1.05 ± 0.03 (10 μM)	−2.338
	4-4	4′Cl	7.8 ± 1.2	1.24 ± 0.09 (25 μM)	−2.309
	4-5	2′OH	9.4 ± 1.1	1.07 ± 0.03 (25 μM)	−2.023
	4-6	3′OH	11.2 ± 1.5	1.08 ± 0.03 (25 μM)	−2.129
Series 5, 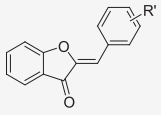	**5-1**	2′OH	≈50[f]	1.40 ± 0.60 (5 μM)	−2.176
Series 6, 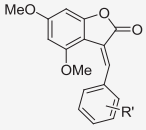	6-1	H	25.2 ± 1.8	1.04 ± 0.08 (25 μM)	−1.874
	6-3	2′OMe	11.6 ± 1.2	1.03 ± 0.05 (25 μM)	−1.715
	6-4	2′Cl	6.4 ± 1.2	0.97 ± 0.09 (10 μM)	−1.997
Series 7, 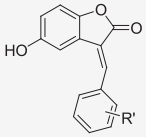	**7-2**	2′OH	2.8 ± 0.5	1.12 ± 0.08 (10 μM)	−2.118
	7-8	4′Cl	3.4 ± 0.2	1.04 ± 0.10 (10 μM)	−2.436
Series 8, 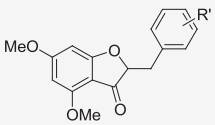	**8-2**	2′OH	≈50[f]	ND[d]	−1.007

Table 2 (*continued*)

Series	Compound	R′ on ring B	CD (μM)[a]	Fold induction of CYP1A1[b]	E_{LUMO} (eV)[c]
Sulphoraphane[g]			0.21 ± 0.02	0.92 ± 0.04 (1 μM)	ND[d]
BNF[g]			0.012 ± 0.05	4.25 ± 0.15 (1 μM)	ND[d]

[a] Only compounds that increased NQO1 activity in Hepa1c1c7 cells by at least 2 fold at 5 μM or 25 μM were evaluated for CD (concentration required to increase NQO1 activity by 2-fold). Mean ± SD for n = 3

[b] Fold induction of CYP1A1 activity in Hepa1c1c7 cells as determined by the EROD assay. Mean ± SD for n = 3. Concentration at which compound was tested is given in parenthesis.

[c] E_{LUMO} values were determined using SPARTAN 2006 on energy minimized structures. Details are given in Section 5.13.

[d] Not determined.

[e] Ring B is replaced by a pyridine ring.

[f] **5-1** and **8-2** did not induce NQO1 activity by 2-fold at the highest concentration tested (25 μM). CD was estimated to be ≈50 μM.

[g] CD values were comparable to those reported by Dinkova-Kostova et al. [36] using the same method.

Next, aurones **1-1**, **1-5**, **2-5**, **5-1**, **8-2** and sulforaphane were investigated for their effects on TrxR, an antioxidant enzyme whose transcription is activated by the Nrf2 pathway [39]. We found that **1-1**, **1-5** and **2-5** significantly induced TrxR activity at 10 μM after 24 h incubation while the inactive NQO1 inducers **5-1** and **8-2** failed to do so under similar conditions (Fig. 6). Sulforaphane caused a modest but significant induction of TrxR activity (1.3 fold). A similar level of TrxR induction was reported for sulforaphane at 12 μM in HepG2 cells [40].

To determine if the induction of TrxR activity was accompanied by an upregulation in TrxR protein expression, lysates from the TrxR activity assays were analyzed by Western blotting for TrxR immunoreactivity and the blots were quantified by densitometry. As shown in Fig. 7, TrxR levels from cells treated with **1-1**, **1-5** and sulforaphane were significantly increased compared to untreated cells.

3.5. Quantitative structure–activity relationship (QSAR) of NQO1 induction activities of aurones and isoaurones

The induction activities of the aurones and related compounds were analyzed by partial least squares projection to latent structures (PLS) and the genetic algorithm (GA) approach to provide a quantitative analysis of structure–activity relationships [41,42]. PLS involves the identification of principal components that can concurrently explain the variance in the descriptor set as well as maximize the correlation to the dependent variable (−log CD or pCD). GA mimics molecular evolution by engaging cycles of variation and selection as driving forces for optimization. Seventeen descriptors related to size, electronic properties and lipophilicity were collected for all compounds but analysis was limited to those compounds with CD values (Table 2) as well as **5-1** and **8-2**. The latter were included to provide a balance between strong inducers and weaker members (**5-1**, **8-2**), as well as to ensure that all series were represented in the analysis.

The thirty-three compounds characterized by 17 descriptors were analyzed by PLS using pCD as dependent variable. A satisfactory one-component model ($p < 0.05$) that could account for 36% (R^2Y) and predict 26% (Q^2) of the variation in activity was obtained. The model was improved by omitting the 4,6-dimethoxyisoaurones of Series 6 (n = 3) because their large residual values ($pCD_{observed} - pCD_{predicted} \geq 0.9$) suggested they were outliers. The resulting one-component model showed improved

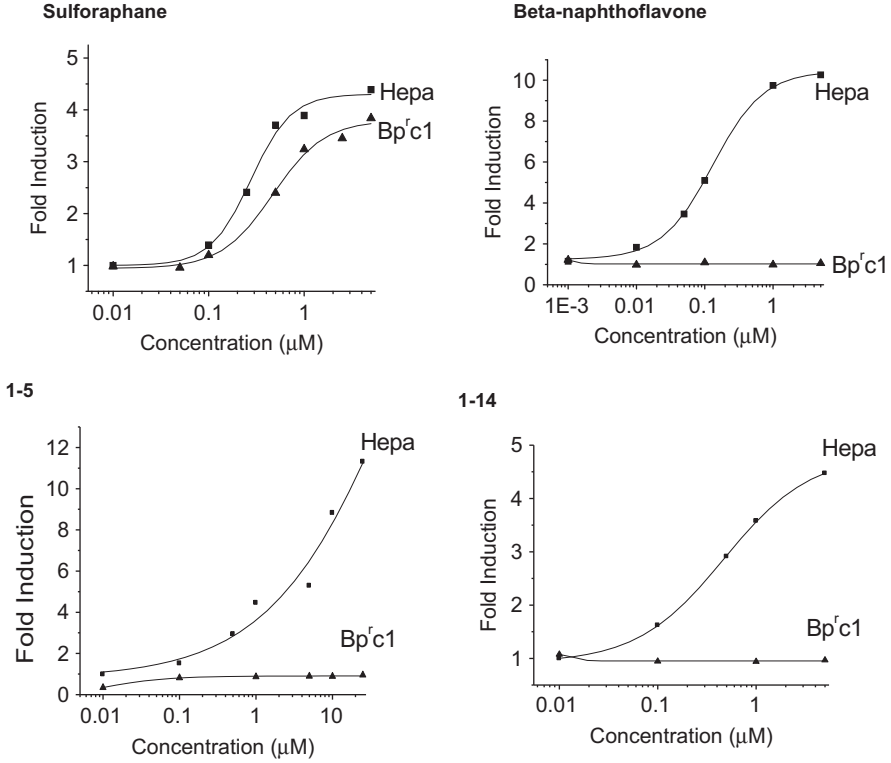

Fig. 2. NQO1 induction in Hepa1c1c7 and BpRc1 cell lines by sulforaphane, beta-naphthoflavone, **1-5** and **1-14**.

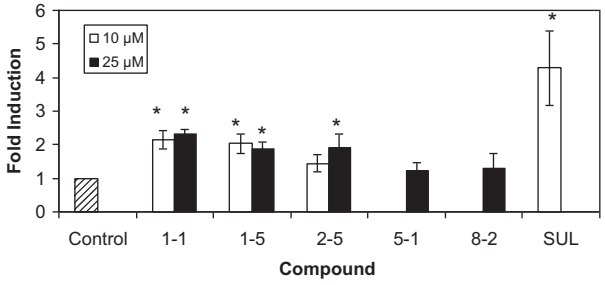

Fig. 3. Induction of luciferase activity of Hepa1c1c7 cells transiently transfected with pGL3-ARE firefly luciferase reporter plasmid and incubated with test compound (10 μM or 25 μM) for 24 h. The fold increase in luciferase activity is represented as the mean and SD of 3 independent replicates of cell transfection and exposure. (*) indicates a response significantly different from the control ($p < 0.05$, independent T-test).

statistics ($R^2Y = 0.586$, $Q^2 = 0.467$). The contribution to activity by the various descriptors is depicted in the coefficient plot (Fig. 8). This figure shows that activity was correlated to size (area, volume), non-polar surfaces (HAS-HYD, ASA) and lipophilicity (Log P) and inversely related to polar surface areas (TPSA, VSA-POL) and to a lesser extent, the number of H bond donors (HD) and acceptors (HA). Electronic descriptors like HOMO, LUMO and dipole moment had negligible effects on activity. Thus, the PLS model identified potent inducers to be those with smaller total polar surface areas, larger VDW areas/volumes and larger hydrophobic VDW surface areas.

To assess the validity of the model, the 30 compounds were randomly divided into a training set (n = 16) and a test set (n = 14). A model was generated with the training set using the same descriptors as before and it was used to predict the activity of the test set. A reasonable error of prediction (RMSEP) of 0.382 was obtained for the test set.

Next, the induction activities of the 33 compounds were analyzed by GA using the same descriptors. Models were generated by the fixed and variable length approaches. The best equation from each approach is given in Equations (1) and (2). Variable length GA was preferred because it gave a simpler model with fewer descriptors (Equation (2)).

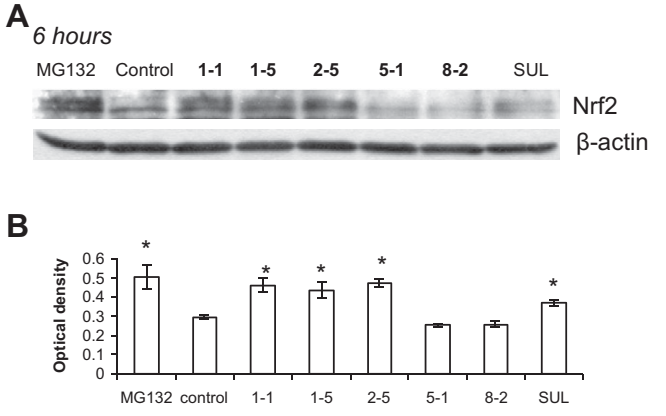

Fig. 4. Immunoblot analysis of Nrf2 protein. (A) Western blot analysis of Hepa1c1c7 cell lysates probed with Nrf2 antibody. Test compounds (10 μM), MG132 (25 μM) and sulforaphane (SUL, 10 μM) were incubated with Hepa1c1c7 cells for 6 h. MG132 is a proteosome inhibitor and causes the accumulation of Nrf2. Immunoblots shown were representative of 3 experiments. (B) Quantitation of immunoblots by image densitometry. (*) indicates that the intensity of the blot is greater than that of control ($p < 0.05$, independent T-test).

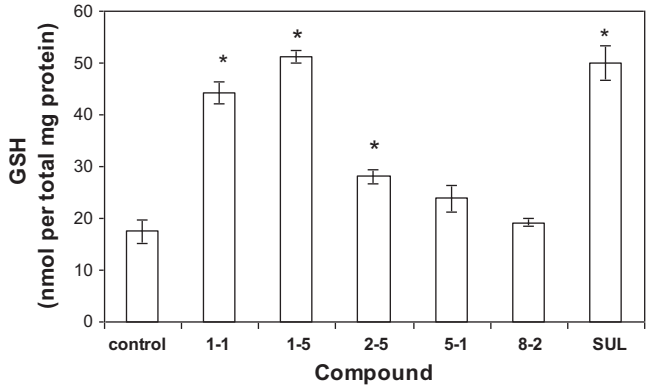

Fig. 5. GSH levels (expressed as nmol per total mg protein) in Hepa1c1c7 cells incubated with aurones and sulforaphane (SUL) at 10 μM, 24 h. Values are mean ± SEM (n = 3). * Indicates significant elevation of GSH compared to control cells ($p < 0.05$, 1-way ANOVA with Dunnett as posthoc test).

Fixed length:

$$\begin{aligned} \text{pCD} = {} & 4.74 - 2.10E_{\text{LUMO}} - 2.52\ \text{Log}\ P \\ & - 0.66[\text{VDW surface area of H bond acceptor}] \\ & + 0.08[\text{Hydrophobic VDW surface area}] \end{aligned} \quad (1)$$

RMSE = 0.487, $R^2 = 0.522$, R^2 (adjusted) = 0.454, AIC (Akaike information criterion) = 59.19, LOF (Lack of Fit) = 0.414, F = 7.64

Variable length:

$$\begin{aligned} \text{pCD} = {} & -4.75 - 1.55E_{\text{LUMO}} \\ & + 0.014[\text{Water accessible surface area}] \end{aligned} \quad (2)$$

RMSE = 0.552, $R^2 = 0.387$, R^2 (adjusted) = 0.346, AIC = 62.40, LOF = 0.394, F = 9.45.

Validation was carried out using the same training and test sets described for PLS, except that the Series 6 compounds were not omitted and one extra member (**6-1**) was included in the training set (n = 17). Equations were generated with variable length GA and leave-one-out validation. As GA uses an "evolutionary" approach to generate models, different equations were obtained for each run. These equations differed in the type of descriptors identified but consistently gave a high weight to the E_{LUMO} term. Equation (3) is an example:

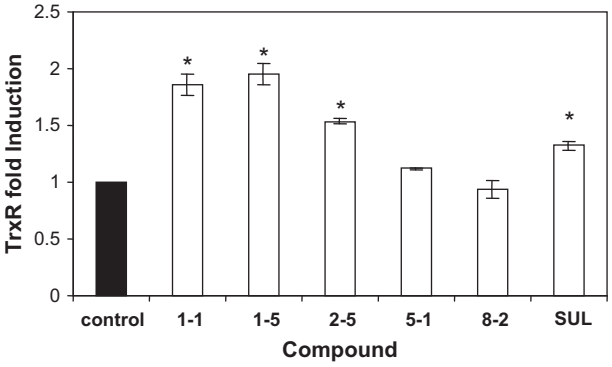

Fig. 6. Induction of TrxR activity by test compounds and sulforaphane (SUL) at 10 μM, 24 h incubation in Hepa1c1c7 cells. Fold induction is measured by the ratio of absorbances of treated cells versus control cells. Mean ± SEM (n = 3). * indicates significant induction ($p < 0.01$, 1-way ANOVA with Dunnett as posthoc test).

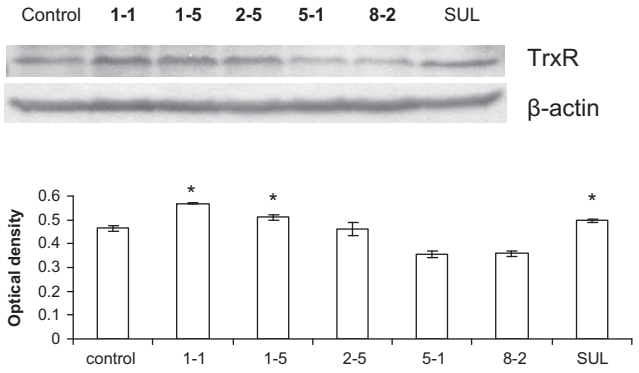

Fig. 7. Immunoblot analysis of TrxR protein. (A) Western blot analysis of Hepa1c1c7 cell lysates probed with the TrxR antibody. Test compounds (10 μM) and sulforaphane (SUL, 10 μM) were incubated with Hepa1c1c7 cells for 24 h. Immunoblots shown were representative of 3 experiments. (B) Quantitation of immunoblots by image densitometry. (*) indicates that the intensity of the blot is greater than that of control ($p < 0.05$, independent T-test).

$$\begin{aligned} \text{pCD} = & -5.50 - 1.94E_{\text{LUMO}} \\ & + 0.023[\text{water accessible surface area}] \\ & - 0.59[\text{molar refractivity}] \end{aligned} \quad (3)$$

RMSE = 0.527, RMSE (test set) = 0.567, R^2 = 0.487, R^2 (adjusted) = 0.377, AIC = 37.99, LOF = 0.624, F = 4.42.

Unlike PLS, the analysis by GA identified E_{LUMO} as a key contributor to activity. E_{LUMO} represents the energy required for a molecule in the dilute gas phase to accept an electron. Compounds with lower E_{LUMO} energies have greater affinities for electrons and are stronger oxidizing agents. An inverse relationship was predicted between activity (pCD) and E_{LUMO} which meant that potent NQO1 inducers were compounds that had low lying E_{LUMO} and were ready acceptors of electrons.

When the E_{LUMO} values of the compounds were compared, it was noted that **8-2** had the lowest LUMO energy and that the variation in E_{LUMO} values of the other compounds did not adequately reflect the variation in their CD values (Table 2). For example, **5-1** which was the other poor NQO1 inducer (CD estimated to be 50 μM) included in the analysis, had an E_{LUMO} (−2.17 eV) that was comparable to other potent inducers (**2-2**, **3-3**, **3-5**). Thus, it may be that the low E_{LUMO} value of **8-2** coupled with its negligible NQO1 induction activity influenced the outcome of the GA analysis. To test this possibility, the analysis was repeated without **8-2**, and with other conditions unchanged. Indeed, we found that the resulting model no longer included E_{LUMO} as a descriptor (Equation (4)). It would seem that the usefulness of the E_{LUMO} term is limited to compounds that possess or lack the exocyclic double bond but it is not an adequate gauge of induction activity among compounds with intact double bonds.

Variable length:

$$\begin{aligned} \text{pCD} = & -1.91 + 0.031[\text{Water accessible surface area}] \\ & - 0.030[\text{van der Waals area}] \end{aligned} \quad (4)$$

RMSE = 0.542, R^2 = 0.364, R^2 (adjusted) = 0.320, AIC = 59.63, LOF = 0.384, F = 8.31.

4. Discussion

Prior to the present investigation, only two aurones have been reported to induce NQO1 activity in Hepa1c1c7 cells [14]. Both compounds were 6-hydroxyaurones and induced NQO1 to a moderate degree (CD 6–20 μM). We have shown that appropriate functionalization of the aurone template resulted in compounds with markedly improved NQO1 induction properties. Several potent inducers with submicromolar CD values were found among the 4,6-dimethoxyaurones highlighting the potential of this template for future lead optimization.

The aurones are proposed to activate both the AhR/XRE and Keap1/Nrf2/ARE pathways to bring about induction of NQO1. The

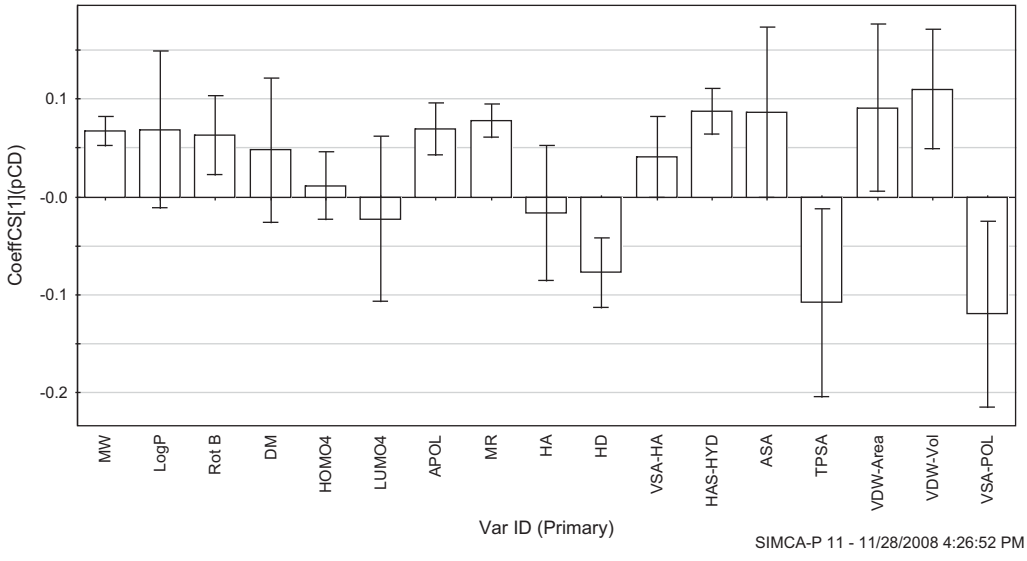

Fig. 8. Coefficient Plot generated by PLS on 30 compounds and 17 descriptors (R^2Y = 0.586, Q^2 = 0.467). Descriptors are represented by columns and the height of each column is directly related to its contribution to activity (pCD). A positive coefficient indicates a direct correlation to activity and a negative coefficient indicates an inverse correlation. MW = molecular weight; Log P = log P (octanol/water); Rot B = number of rotatable bonds; DM = dipole moment; HOMO4 = E_{HOMO}; LUMO4 = E_{LUMO}; APOL = sum of atom polarizations; MR = molar refractivity; HA = number of H bond acceptors; HD = number of H bond donors; VSA-HA = van der Waals' surface areas of H bond acceptors; HAS-HYD = Hydrophobic van der Waals' surface area; ASA = water accessible surface area; TPSA = topological polar surface area; VDW-Area and VDW-Vol = van der Waals' area and volume; VSA-POL = Polar van der Waals' surface area.

involvement of the AhR/XRE pathway was seen from (i) the failure of the target compounds to induce NQO1 activity in mutant Bp^{r}c1 cells that lacked functional Ah-receptors and (ii) their ability to induce CYP1A1 activity in Hepa1c1c7 cells. The involvement of the Nrf2/ARE pathway was seen from the ability of selected aurones (**1-1**, **1-5**) to (i) increase the luciferase activity of Hepa1c1c7 cells transiently transfected with a reporter gene under expression regulation of an ARE from the human NQO1 gene, (ii) increase Nrf2 levels in Hepa1c1c7 cells and (iii) induce TrxR expression (with increase in enzyme activity) and increase GSH content in Hepa1c1c7 cells. The failure of aurones (**5-1** and **8-2**) that were poor NQO1 inducers to affect these processes under similar conditions lend further support to the contribution of Nrf2/ARE signaling to the NQO1 induction process.

The involvement of two pathways for the induction of NQO1 raises the question as to whether aurones affected both routes to the same degree. The present findings suggest a greater role for the AhR/XRE pathway as seen from the failure of the aurones to induce NQO1 activity in mutant Hepa1c1c7 cells that were defective in AhR signaling. Moreover, the more potent aurones (**1-1**, **1-5**) caused only modest increases in luciferase activity which was regulated by Nrf2/ARE signaling. A larger increase, closer to that observed for sulforaphane under similar conditions, would be expected if these aurones induced NQO1 activity primarily or exclusively by the Nrf2/ARE pathway. Additional investigations using reporter cell lines that are stably transfected with a firefly luciferase reporter gene under expression regulation of an ARE or XRE-containing sequence from relevant genes would provide a clearer assessment of the relative contributions of these two pathways. Using these stably transfected cell lines, Lee-Hilz and co-workers demonstrated that at physiologically relevant concentrations, some flavonoids (quercetin, fisetin and some hydroxylated flavones) induced ARE-mediated gene expression to a greater degree than XRE-mediated gene expression [22].

The present findings support a mixed activator status for aurones, not unlike that reported for other flavonoids like quercetin and chrysin [7,27]. It has been argued that mixed activators have greater chemopreventive potential than mono- or bifunctional inducers. Pretreatment of human colon LS-174 cells by a combination of indolo[3,2-b]carbazole (a bifunctional inducer) and sulforaphane (a monofunctional inducer) provided substantial protection against the genotoxic effects of benzo[a]pyrene, and this protection was greater than that achieved by either agent alone [43]. Mixed activators chrysin [23] or BNF [24] were stronger inducers of the Phase 2 enzyme UGT1A6 (controlled by both AhR and Nrf2 activated pathways) than TCDD, a selective AhR activator. Alternatively, the results may reflect the coordinated regulation of the AhR and Nrf2 gene batteries that has been expounded by others [44,45]. Proposed links between the two pathways may involve Nrf2 as a target gene of AhR or an indirect activation of Nrf2 by CYP1A1 generated ROS/electrophiles or a direct interaction between AhR/XRE and Nrf2/ARE signaling due to their close proximities in the regulatory regions of NQO1 [44]. Aurones may be agents capable of exploiting the cross-talk between the AhR and Nrf2 gene batteries by mechanisms that remain to be understood.

The structural features associated with NQO1 induction activity was investigated in some detail. The strong representation of potent inducers from the 4,6-dimethoxyaurones of Series 1 compared to the other series emphasized the need for a substituted ring A, preferably one with bulky and lipophilic groups. This was corroborated by PLS which identified non-polar size parameters like van der Waals' area/volume and hydrophobic surface area as important contributors to activity. Another crucial feature was the exocyclic double bond as seen from the loss of activity when the double bond was reduced (Series 8) or omitted (**1-27**, **2-16**). This feature was not identified by any of the descriptors in the PLS analysis but it was captured by the E_{LUMO} term in the GA approach. This raises the question as to what aspect of the double bond is actually reflected by E_{LUMO}. By its definition, this should be the electron affinity (electrophilicity) of the double bond and the Michael acceptor of which it is a part. We have shown that the aurones activated the Nrf2/ARE pathway and accordingly, their reactivities as inducers should be strongly linked to the electron affinity of the Michael acceptor moieties. However this proposal is framed with several caveats. First, we were not able to demonstrate the reaction of Series 1 aurones with electron rich thiol reagents like GSH and N-acetylcysteine (unpublished results). Flavonoids also failed to show electrophilic activity but they produced electrophilic metabolites that could react with glutathione or DNA [46,47]. Second, other QSAR studies on NQO1 induction activity recognized E_{HOMO} and not E_{LUMO} as a key descriptor [46,48,49]. In these reports, compounds that were good donors of electrons (high E_{HOMO}) were more potent inducers. The role of E_{HOMO} was explained by the involvement of active metabolites that mediated the actual biological response. Lee-Hilz and co-workers postulated that flavonoids with a catechol moiety were oxidized to quinones or semiquinones which were the reactive species [46]. In a study of diphenols, a 2-step mechanism of NQO1 induction was proposed involving an initial oxidation of the diphenol inducer to its quinone and the subsequent oxidation of reactive thiol groups in a protein involved in NQO1 induction by these quinones [49]. E_{HOMO} of these compounds would then reflect the ease with which electron donation occurs to give these active species. As the 1,4- or 1,2-diphenolic motif involved in quinone formation is not found in the present series of compounds (except **1-8**), a correlation to E_{HOMO} would not be anticipated.

Besides electrophilicity, the E_{LUMO} term could reflect the role of olefinic double bond in influencing the conformation of the target compound. Reduction of the double bond causes a loss in planarity and greater conformational flexibility for ring B. This feature may not be adequately captured by the existing descriptors used in the QSAR analysis and E_{LUMO} may indirectly reflect the conformational change. The importance of conformational planarity was highlighted by the failure of the non-planar flavonoid taxifolin to activate ARE-mediated gene expression compared with other planar flavonoids like quercetin and fisetin [50]. The explanation was that interaction with Keap1 or other effector/receptor protein involves a stereospecific interaction which was diminished in a non-planar compound.

The structure–activity relationships deduced in this study would contribute to lead optimization of aurones to give more potent chemopreventive agents. It also provides insight into the structural requirements of agents that activate both the AhR/XRE and Nrf2/ARE signaling pathways. Planarity and size are important components for interaction with the AhR [51] and these features are evident among the aurones/isoaurones. The reactivity of the Michael reaction acceptor is a prominent feature of NQO1 inducers that activate the Nrf2/ARE pathway but the present results do not conclusively support the involvement of this moiety as an electrophile.

In conclusion, this study has highlighted several desirable features of aurones as inducers of chemopreventive Phase II enzymes, namely their potencies as inducers of NQO1 as seen from the submicromolar CD values of several 4,6-dimethoxyaurones and their ability to activate both AhR and Nrf2 gene/protein batteries. An analysis of structure–activity trends highlighted a stereo-electronic role for the exocyclic double bond (for conformational planarity and/or electrophilicity) and a substituted ring A to maintain steric bulk and lipophilicity.

5. Experimental

5.1. General details

Reagents (synthetic grade or better) were obtained from Sigma–Aldrich Chemical Company Inc (Singapore) and used without further purification. Melting points were determined on a Gallenkamp melting point apparatus and reported as uncorrected values. Nominal mass spectra were captured on an LCQ Finnigan MAT equipped with a chemical ionization (APCI) probe and *m/z* values for the molecular ion were reported. HRMS were taken using a Q-TOF Premier (Waters Corp., Milford, USA). ^{1}H and ^{13}C NMR spectra were determined on a Bruker Spectrospin 300 Ultrashield spectrometer and referenced to TMS (for ^{1}H NMR spectra). Merck silica 60 F254 sheets and Merck silica gel (0.040–0.063 mm) were used for thin layer chromatography (TLC) and flash chromatography respectively. Purity of final compounds were verified by combustion analysis (C,H) on a Perkin Elmer PRE-2400 Elemental Analyzer or by high pressure liquid chromatography (compound **6-2**). Spectroscopic and other analytical data of final compounds are given in Supplementary Information.

5.2. General procedure for the synthesis of series 1

3,5-Dimethoxyphenoxyacetic acid (**1-28**) and 4,6-dimethoxybenzofuran-3(*2H*)-one (**1-27**) were synthesized as described earlier [25,34]. To a solution of **1-27** (100 mg, 0.52 mmol) in methanol (10 ml) was added the substituted benzaldehyde (0.76 mmol), followed by a solution of KOH (500 mg, 8.92 mmol) in distilled water (1 ml). The solution was stirred at room temperature for 1–3 h. The desired compound was obtained as a precipitate, removed by suction filtration, washed with cold methanol and crystallized in ethanol or methanol to give the purified aurones. In cases where the compounds did not precipitate, the reaction mixture was quenched with dilute HCl and extracted with ethyl acetate (3 × 20 ml). The organic phase was washed with brine, dried over $MgSO_4$, and evaporated in *vacuo* to yield crude products which were purified by column chromatography with hexane:ethyl acetate as eluting solvents.

5.3. General procedure for the synthesis of series 2

5.3.1. 2′, 4′, 6′-Trihydroxy-2-chloroacetophenone (**2-17**) [29]

2-17 was prepared according to the method of Beney et al. [29]. It was obtained in 39% yield, mp 208–210 °C; ^{1}H NMR (DMSO-d_6, 300 MHz): δ 4.96 (s, CH_2), 5.81 (s, 2H), 10.5 (s, 1H), 12.0 (s, 2H, –OH).

5.3.2. 4, 6-Dihydroxybenzofuran-3(2H)-one (**2-16**) [29]

2-17 (5 mmol) was dissolved in methanol (30 ml), treated with NaOAc (14 mmol) and refluxed (2 h). The solvent was removed in vacuo to give a residue that was diluted in water, extracted with diethyl ether, washed with brine and dried with Na_2SO_4. On removal of the solvent under reduced pressure, **2-16** was obtained as a brown solid in 88% yield, Mp 211–212 °C (lit. [29] mp 210–212 °C). ^{1}H NMR (Methanol-d_4, 300 MHz): δ 4.59 (s, 2H), 5.91 (d, J = 1.5 Hz, H_5), 5.97 (d, J = 1.9 Hz, H_7); ^{13}C NMR (Methanol-d_4, 75 MHz): δ 74.8, 90.1, 96.2, 99.6, 102.6, 157.5, 167.6, 175.6, 193.9; MS (APCI) *m/z* $[M+1]^+$ 167.2.

5.3.3. Condensation of **2-16** with substituted benzaldehydes

To a solution of **2-16** in methanol (10 ml/mmol) was added the substituted benzaldehyde (0.76 mmol), followed by a solution of KOH 50% in water (1.5 ml/mmol) and heated in a dedicated microwave reactor (Biotage Initiator) at 110 °C for 10–15 min. The reaction mixture was quenched with dilute HCl and extracted with ethyl acetate (3 × 20 ml). The organic phase was washed with brine, dried over Na_2SO_4, and evaporated in vacuo to yield crude products which were purified by column chromatography using hexane:ethyl acetate (9:1) as eluting solvents.

5.4. General procedure for the synthesis of series 3

5.4.1. 5-Hydroxybenzofuran-3(2H)-one (**3-14**)

The method of King and Ostrum [30] was followed. Briefly, a solution of 2′, 5′-dihydroxyacetophenone (16.4 mmol) in ethyl acetate (20 ml) and chloroform (20 ml) was added to $CuBr_2$ (33 mmol) contained in a round bottom flask under a blanket of N_2. The reaction mixture was refluxed (8 h) with vigorous stirring after which reduced copper (I) bromide was filtered off and the filtrate evaporated in vacuo to give 2-bromo-1-(2,5-dihydroxyphenyl) ethanone (**3-13**) as an amber oil which was used without further purification. Crude **3-13** was dissolved in methanol (10 ml), treated with 0.5 ml of KOH (50% in distilled water) and refluxed (2 h). The solvent was removed in vacuo and the residue purified by column chromatography (hexane:ethyl acetate = 8:1) to give **3-14** as a light yellow solid, mp 133–135 °C (lit [52] mp 152–153 °C) 55% yield. ^{1}H NMR (DMSO-d_6, 300 MHz): δ 4.74 (s, 2H), 6.86 (d, J = 2.3 Hz, H_4), 7.12 (d, J = 9 Hz, H_7), 7.18 (dd, J_1 = 2.3 Hz, J_2 = 11 Hz, H_6); ^{13}C NMR (DMSO-d_6, 75 MHz): δ 75.1, 106.3, 114.1, 121.1, 126.7, 152.3, 167.2, 199.9; MS (APCI) *m/z* $[M+1]^+$ 151.2.

5.4.2. Condensation of **3-14** with substituted benzaldehydes

The procedure described in Section 5.3.2 was followed except that **3-14** was reacted with the benzaldehyde by heating in an oil bath at 60 °C for 1 h.

5.5. General procedure for the synthesis of series 4

5.5.1. 6-Hydroxybenzofuran-3(2H)-one (**4-14**)

The procedure described in Section 5.4.1 was followed except that 2′, 4′-dihydroxyacetophenone was the starting material. The intermediate 2-bromo-1-(2,4-dihydroxyphenyl) ethanone (**4-13**) was also used for the next step without purification. **4-14** was obtained as a light yellow solid in 21% yield. Mp 242–244 °C (lit. [53] mp 245 °C). ^{1}H NMR (DMSO-d_6, 300 MHz): δ 4.70 (s, 2H), 6.50 (d, J = 1.5 Hz, H_7), 6.61 (dd, J_1 = 1.9 Hz, J_2 = 10 Hz, H_5) 7.48 (d, J = 8.3 Hz, H_4), 10.9 (br s, –OH); ^{13}C NMR (DMSO-d_6, 75 MHz): δ 80.8, 101.0, 108.1, 115.6, 131.1, 163.2, 166.3, 198.4; MS (APCI) *m/z* $[M+1]^+$ 151.1

5.5.2. Condensation of **4-14** with substituted benzaldehydes

The procedure described in Section 5.4.2 was followed.

5.6. General procedure for the synthesis of series 5

Benzofuran-3(2*H*)-one was purchased and reacted with 2-hydroxybenzaldehyde or 2-chlorobenzaldehyde as described in Section 5.4.2 to give the desired products.

5.7. General procedure for the synthesis of series 6

5.7.1. 4, 6-Dimethoxy-2-hydroxyphenylacetic acid (**6-6**) [31]

Briefly, 4,6-dimethoxy-2-hydroxyacetophenone (1 g, 5 mmol) was heated with sulphur (0.24 g, 7.5 mmol) and morpholine (1.2 ml, 7.5 mmol) at 150 °C, 24 h. The reaction mixture was taken into dichloromethane, and washed successively with brine and dilute HCl. On removal of solvent, the residue was crystallized in ethanol to give the thiomorpholide which was hydrolyzed by refluxing (6 h) in 2 M NaOH. The solution was then neutralized with 1 N HCl, extracted with diethyl ether, the organic layer washed with

brine and dried with Na_2SO_4. On removal of solvent *in vacuo*, **6-6** was obtained in 16% yield. White crystals, mp 140–142 °C (lit [31] mp 140–140.5 °C); ^{1}H NMR ($CDCl_3$, 300 MHz): δ 3.69 (s, CH_2), 3.76 (s, OCH_3), 3.79 (s, OCH_3), 6.10 (s, 1H), 6.11 (s, 1H).

*5.7.2. 4, 6-Dimethoxybenzofuran-2(3H)-one (**6-7**) [31]*

A mixture of **6-6** (0.5 g, 2.35 mmol) and phosphorus oxychloride (2 ml) in dichloroethane (20 ml) was stirred at room temperature, 18 h, after which the reaction mixture was diluted with distilled water and extracted with dichloromethane. The organic layer was washed successively with dilute $NaHCO_3$, water and brine, and dried with $MgSO_4$. The solvent was removed *in vacuo* and the residue was purified by column chromatography with hexane:ethyl acetate (5:1) to give **6-7** as a white solid in 80% yield, mp 155–156 °C (lit.[31] mp 154 °C) ^{1}H NMR ($CDCl_3$, 300 MHz): δ 3.60 (s, 2H), 3.81 (s, OCH_3), 3.82 (s, OCH_3), 6.22 (d, J = 1.8 Hz, 1H), 6.32 (d, J = 1.8 Hz, 1H); ^{13}C NMR ($CDCl_3$, 75 MHz): δ 30.8, 55.5, 55.7, 89.4, 94.2, 102.3, 155.8, 156.1, 161.6, 174.8; MS (APCI) m/z $[M+1]^+$ 194.7.

*5.7.3. Condensation of **6-7** with substituted benzaldehydes*

A solution of **6-7** (50 mg, 0.25 mmol) in acetic anhydride (5 ml) was added with 1.5 ml of triethylamine and the substituted benzaldehyde (0.5 mmol). The mixture was heated at 60 °C for 6–12 h. TLC was used to monitor if reaction was completed. Thereafter, the mixture was diluted with water, refluxed (20 min), cooled and extracted with dichloromethane (3 × 20 ml). The organic layer was then washed, dried with $MgSO_4$ and removed under reduced pressure to give the crude product which was purified by column chromatography with hexane:ethyl acetate 8:1.

5.8. General procedure for the synthesis of series 7

Commercially purchased 5-hydroxy-2-benzofuran-2-(*3H*)-one (100 mg, 0.67 mmol) was dissolved in ethanol (10 ml), treated with 1.5 ml of ethanolic KOH (4 g in 100 ml) and the substituted benzaldehyde (1.3 mmol). The reaction mixture was stirred at room temperature for 12 hours after which the mixture was diluted with dilute HCl and extracted with ethyl acetate (3 × 30 ml). The organic fractions were washed with brine and dried with Na_2SO_4. The solvent was evaporated to yield the crude product which was purified by column chromatography with hexane:ethyl acetate (5:1) as eluting solvents.

*5.9. General procedure for the synthesis of series 8 (**8-1**, **8-2**)*

1-1 or **1-5** (80 mg, 0.3 mmol) was dissolved in methanol (50 ml) and 10 mg of 10%Pd/C was added under a blanket of N_2. Reaction with H_2 (40 psi) was carried out in a Parr hydrogenator with agitation for 24 h. At the end of the reaction, the catalyst was removed by filtration and the filtrate was evaporated under reduced pressure to give the crude product as an oily residue. The desired product was obtained after purification by column chromatography with hexane:ethyl acetate (5:1) as eluting solvents.

*5.10. Protection and deprotection of phenolic hydroxyl groups of **2-16** [26]*

A solution of **2-16** (3 mmol) and N, N-diisopropylethylamine (2 equiv) in anhydrous DMF was cooled to 0 °C. 2-Methoxyethoxymethyl chloride (MEM Cl, 2 equiv) was added dropwise and the reaction mixture was stirred at room temperature, 30 min. The mixture was then diluted with water and extracted with ethyl acetate (3 × 60 ml). The organic fractions were washed, dried with Na_2SO_4 and evaporated *in vacuo* to yield the product was an oil. It was used without further purification for condensation with the benzaldehyde (2-fluorobenzaldehyde or 3-methoxy-4-hydroxybenzaldehyde). At the end of the reaction, the protecting groups were removed by adding ethereal HCl to acidify the methanolic solution and heating at 60 °C for another 2 h. The reaction mixture was diluted with water and extracted with ethyl acetate (3 × 20 ml), after which the organic phase was washed with brine, dried over Na_2SO_4, and evaporated *in vacuo* to yield the crude product which was purified by column chromatography as described earlier.

5.11. Protection and deprotection of phenolic hydroxyl groups on 3-hydroxybenzaldehyde, 4-hydroxybenzaldehyde, 2, 3-dihydroxybenzaldehyde and 2,4-dihydroxybenzaldehyde

The benzaldehyde (3 mmol), pyridinium p-toluenesulphonate (50 mg, 0.2 mmol) and 3,4-dihydro-2*H*-pyran (673 mg, 8 mmol) were dissolved in dichloromethane (10 ml) and stirred for 4 h at room temperature. The reaction mixture was then washed with 1 M Na_2CO_3 (3 × 20 ml), dried over anhydrous Na_2SO_4 and the solvent removed in vacuo to give the crude tetrahydropyranyl ether as oil. It was used without purification for the condensation with the benzofuranone as described in earlier paragraphs. At the end of the reaction, deprotection was carried out by acidifying the reaction mixture with 4 M HCl and stirring for 4 h at room temperature. The reaction mixture was extracted with ethyl acetate and worked up as described earlier.

5.12. Biological evaluation

5.12.1. General details

Glutathione (reduced), 5-sulfosalicylic acid, 5,5′-dithiobis-(2-nitrobenzoic acid) (DTNB), bovine insulin, yeast glutathione reductase, sulforaphane, beta-naphthoflavone (BNF), yeast glucose-6-phosphate dehydrogenase, menadione, dicoumarol, 7-ethoxyresorufin and salicylamide were purchased from Sigma–Aldrich, Singapore. Human thioredoxin protein was obtained from Imco Corporation (Stockholm, Sweden, www.imcocorp.se). Bradford dye concentrate was from Bio-Rad Laboratories (Hercules, CA, USA). Chemicals and reagents for cell-based assays and cell culture were purchased from Sigma–Aldrich Pte Ltd, Singapore. Hepa1c1c7 and Bp^rc1 cell lines were obtained from the American Type Culture Collection (Rockville, MD, USA). Primary antibodies against Nrf2 and TrxR were purchased from Santa Cruz Biotechnology Inc. (Santa Cruz, CA, USA). Antibody against β-actin was obtained from Sigma–Aldrich, Singapore. Dual Luciferase Assay System® and pRL-CMV vector were purchased from Promega Pte Ltd, Singapore. Test compounds were dissolved in DMSO and were diluted with medium so that the final concentration of DMSO did not exceed 0.5%.

5.12.2. Cell culture

Mouse hepatoma Hepa1c1c7 and Bp^rc1 cell lines were grown in 75 cm^3 flasks in a humidified, 5% CO_2 incubator at 37 °C. Growth medium was α-minimal essential medium (α-MEM, Invitrogen Corp., CA, USA) supplemented with 100 U/ml penicillin G sodium, 100 μg/ml streptomycin sulfate, and 10% fetal bovine serum (Hyclone, UT, USA). Fetal bovine serum was treated with 1 g/l of activated charcoal and heated at 55 °C for 1.5 h before addition to medium. Cells were sub-cultured when they reached 80–90% confluency and passage numbers 4–20 were used for experiments.

5.12.3. Procedure for NQO1 induction assay [54]

Cells were grown for 24 h in 96-well microtitre plates at a density of 10^4 cells per well and subsequently incubated with test compounds for 48 h, after which the media was decanted and the cells lysed by incubation (10 min) with a solution (50 μl per well) of 0.8% w/v digitonin and 2 mM EDTA, after which the lysed cells were gently agitated (10 min) prior to the addition of a freshly prepared

reaction cocktail of the following composition: 0.5 M Tris–Cl (pH 7.4) (2.5 ml), bovine serum albumin (33 mg), 150 mM glucose-6-phosphate (330 μl), 7.5 mM FAD (33 μl), 50 mM NADP (90 μl), yeast glucose-6-phosphate dehydrogenase (100 units), MTT (15 mg) and deionized water to give a final volume of 50 ml. Menadione (1 μl of 50 mM stock in acetonitrile per ml reaction mixture) was added just before the reaction mixture (200 μl per well) was dispensed into the wells. Five minutes after the addition of the reaction mixture, the reaction was quenched by the addition of 0.3 mM dicoumarol in 0.5% DMSO and 5 mM K_3PO_4 pH 7.4 (50 μl per well). A blue color due to the formation of formazan was observed in each well and its absorbance was measured at 590 nm on a microplate reader (Infinite M200, Tecan AG, Switzerland). Blank wells were similar to treated wells except for the exclusion of cells and control wells were similar to treated wells except for the absence of test compound. The content of DMSO in blank and control wells were 0.5% v/v. NQO1 induction activity of test compound at a given concentration was determined from the equation: Degree of induction $= A_{\text{test compound}} - A_{\text{blank}}/A_{\text{control}} - A_{\text{blank}}$ where A is absorbance of formazan measured at 590 nm.

Sulforaphane and BNF were determined under similar conditions as positive controls. The results were plotted (degree of induction versus concentration) with OriginPro 7.5 (OriginLab Corp., MA) and the concentration of test compound required to increase the basal NQO1 activity by two fold (CD) was determined. CD was reported as mean ± SD from 3 separate determinations.

5.12.4. Determination of 7-ethoxyresorufin-O-deethylase (EROD) activity in Hepa1c1c7 cells [55]

Hepa1c1c7 cells were grown at a density of 10^4 cells per well in a 96-well plate for 24 h. The cells were incubated with test compound for 48 h, after which the medium was removed, the cells washed with 200 μl of PBS and then incubated (37 °C, 40 min) with 5 μM 7-ethoxyresorufin and 2 mM salicylamide in 200 μl of medium. The fluorescence of resorufin was measured at $\lambda_{\text{excitation}}$ of 530 nm and $\lambda_{\text{emission}}$ of 590 nm on a fluorometer. The readings of empty wells (no cells, "blank") and wells with Hepa1c1c7 cells in medium containing 0.5% DMSO but without test compound ("control") were also determined. BNF and sulforaphane were used as controls.

CYP1A1 induction activity was given by the expression:

$$\text{Degree of induction} = F_{\text{Cells+test compound}} - F_{\text{Blank}}/F_{\text{Control}} - F_{\text{Blank}}$$

5.12.5. Determination of the cytotoxicity of test compounds by the microculture tetrazolium (MTT) assay [56]

The MTT assay was performed to obtain the cytotoxicity profiles of the test compounds. Briefly, Hepa1c1c7 cells were grown in 96-well plates at 10^4 cells/well for 24 h. The cells were then incubated with 5 or 25 μM test compounds for 48 h after which the media was decanted. 100 μl of MTT solution (0.5 mg/ml) was added into each well and the plate was incubated at 37 °C for 3 hours. The contents of the wells were decanted and 150 μl of DMSO was added into each well to dissolve the purple formazan crystals. Cell viability was measured by the expression:

$$\text{Cell survival (\%)} = \left[\left(A_{\text{cells+test compound}} - A_{\text{blank}}\right)\Big/ \times \left(A_{\text{untreated cells}} - A_{\text{blank}}\right)\right] \times 100$$

where A is the absorbance of formazan measured at 590 nm in the test ($A_{\text{cells + test compound}}$), control ($A_{\text{untreated cells}}$) or blank ($A_{\text{blank}}$) wells. Each concentration of test compound was evaluated on 3 separate occasions.

5.12.6. ARE-dependent luciferase reporter assay

ARE reporter assays were carried out using a pGL3-ARE firefly luciferase reporter plasmid constructed by Dhakshinamoorthy and Porter [37]. Briefly, Hepa1c1c7 cells were cultured in 12-well plates. At approximately 50% confluency, the cells were co- transfected with pGL3-ARE (1.2 μg) and pRL-CMV (10 ng, Promega Pte Ltd, Singapore) as an internal control for transfection efficiency, using GeneJuice® transfection reagent (Merck KGaA, Darmstadt, Germany) that was premixed in serum-free medium. After 24 h, the transfection medium was replaced by culture medium and the cells were incubated for 12 h in the presence of the test compound. Firefly and renilla luciferase activities were assayed using the Dual Luciferase Assay System® from Promega in accordance to the recommended protocol. Means and standard deviations were based on three independent replicates of cell transfection experiments and subsequent exposure.

5.12.7. Effect of test compounds on total GSH content of Hepa1c1c7 cells [57]

Hepa1c1c7 cells were grown in 10-cm diameter tissue culture plates at a density of 10^6 cells/plate for 24 h. The cells were then incubated with test compounds (final concentration of 10 μM) for 24 h. Each compound was tested in duplicate on separate plates, with one plate used for GSH determination and the other for protein determination. After 24 h, the cells were trypsinized and the media containing detached and trypsinized cells were pooled and pelleted by centrifugation (320 *g*, 5 min). The pellets were washed with ice-cold PBS and treated with 3% w/v 5-sulfosalicylic acid (1 ml). The contents were vortexed and centrifuged (10^5 *g*, 5 min) to remove precipitated proteins. Total GSH content was assayed by following the change in absorbance at 412 nm over 5 min in a cuvette volume of 1 ml containing a final concentration of 0.6 mM DTNB, 0.2 mM NADPH, 10 μg/ml GSH reductase and 20 μl of sample in 0.1 M sodium phosphate-5 mM EDTA buffer. The content of GSH in the supernatant was determined from a calibration plot constructed using five GSH concentrations (0.125–1.5 nmol/200 μl 0.01 M HCl). For the determination of protein content, the cells were lysed with digitonin and 2 mM EDTA as described in Section 5.12.3 and subjected to the Bradford method [58].

5.12.8. Preparation of cell lysates for the TrxR assay and western blots

Hepa1c1c7 cells were grown in 10-cm diameter tissue culture plates at a density of 1 to 2×10^5 cells/ml for 24 h. The cells were incubated with test compounds (10 μM) for 24 h (5% CO_2, 37 °C) after which they were trypsinized and pelleted by centrifugation (320 *g*, 5 min). Cell pellets were lysed in a freshly prepared lysis solution made up of 0.8% w/v digitonin, 2 mM EDTA, and protease inhibitor cocktail (Roche Diagnostics, Mannheim, Germany). The lysate was incubated at 37 °C for 10 min and then gently agitated for another 10 minutes prior to collection of supernatant from cell debris by centrifugation. Total protein concentration of the lysate was then determined by the Bradford method.

5.12.9. Effect of test compounds on thioredoxin reductase (TrxR) activity

TrxR activity was measured in 96-well plates using an end point insulin reduction assay as described by Arner and Holmgren [59]. Briefly, 25 μg of cell lysate was incubated in a final reaction volume of 50 μl containing 85 mM HEPES (pH 7.6), 0.3 mM insulin, 660 μM NADPH, 2.5 mM EDTA, and 5 μM human thioredoxin for 20 min at 37 °C. Background controls involved incubating cell lysates under similar conditions except without human thioredoxin. The reaction

was then quenched by adding 250 μl of 1 mM DTNB in 6 M guanidine hydrochloride - 200 mM Tris–HCl, pH 8.0 solution. The free thiols generated from the insulin reaction were reacted with DTNB to give the reduced product TNB, the absorbance of which is measured at 412 nm. TrxR activity was determined by subtracting absorbance due to the background control from that obtained with the treated lysates.

5.12.10. Western blot of Nrf2 and TrxR

Cell lysates (50 μg total protein) were fractionated on 15% SDS-PAGE gel, transferred to nitrocellulose membranes (Bio-Rad Laboratories Pte Ltd, Singapore), and blocked with 10% non-fat milk in Tris-buffered saline containing 0.05% Tween 20. The membranes were blotted with primary antibodies at room temperature for 3–5 h and then incubated with horseradish peroxidase-conjugated secondary antibodies for 1 h. Protein bands were visualized by enhanced chemiluminescence detection reagents (Amersham Pharmacia Biotechnology, UK) and quantified by densitometric measurements with the ImageJ Program (National Institute of Health, Bethesda, USA). At least 3 independent determinations were made for each compound. Actin was used as a control to ensure equal protein loading.

5.13. Molecular modeling

Aurones (Series 1–5) and isoaurones (Series 6, 7) were drawn in the *Z* and *E* configuration respectively and geometry minimized using the Hamiltonian forcefield MMFF94x in MOE (Chemical Computing Group, Montreal, Canada). **8-1** and **8-2** were arbitrarily represented as R isomers because similar descriptor values were obtained for either R or S isomer. The following molecular descriptors were collected for the compounds using the QuaSAR module in MOE:molecular weight (MW), lipophilicity (Log P in octanol/water), number of rotatable bonds (Rot B), dipole moment (DM), molar refractivity (MR), atom polarization (APOL), number of hydrogen bond acceptors (HA), and hydrogen bond donors (HD), topological polar surface area (TPSA), water accessible surface area (ASA), van der Waals surface area of hydrogen bond acceptors (VSA-HA), van der Waals area (VDW-Area) and volume (VDW-Vol), hydrophobic van der Waals surface area (HAS-HYD), polar van der Waals surface area (VDW-Pol). HOMO and LUMO energies (HOMO4 and LUMO4) were calculated using SPARTAN 2006 for Linux server (Wavefunctions Inc., Irvine, CA). Structures initially minimized by MMFF94x in MOE were minimized again using semi-empirical PM3, followed by restricted Hartree-Fock, and a density functional theory (DFT) B3LYP functional using a 6–31G* basis set. E_{HOMO} and E_{LUMO} energies of the final minimized structures were reported. PLS was run on SIMCA-P 11 (Umetrics AB, Umea, Sweden) with default settings. Water accessible surface area, van der Waals area, polar van der Waals surface area and topological polar surface area were transformed to their logarithmic values for this analysis. QSAR by genetic algorithm was carried out with the QuaSAR-Evolution module on MOE with default settings (population 100, generation 50,000, mutation probability 0.5, eugenic factor 100, initial length 4, operant density 4). In the fixed length approach, a limit of 4 descriptors was specified per model. No restriction was placed on the number of descriptors identified in the variable length approach. 100 equations were generated for each run and the 1st equation obtained by either approach was selected as the "best" equation.

5.14. Statistical analysis

Data were analyzed for statistically significant differences using one-way ANOVA followed by Dunnett's posthoc test, or independent T-test (SPSS 15.0 for Windows, Chicago, IL). p values < 0.05 were considered statistically significant.

Acknowledgements

This work was supported by National University of Singapore Academic Research Fund R 148 000 084 112 (to GML). LCY gratefully acknowledged the financial support (research scholarship) from Ministry of Education, Republic of Singapore and National University of Singapore. The authors thank Dr Elias Arner and Dr Qing Cheng of the Medical Nobel Institute for Biochemistry, Karolinska Institute for their kind provision of human thioredoxin and Dr Alan Porter of the Institute of Molecular and Cell Biology, Singapore for providing pGL3-ARE firefly luciferase reporter plasmid.

Appendix. Supplementary information

Supplementary data associated with this article can be found, in the online version, at doi:10.1016/j.ejmech.2010.03.023.

References

[1] M.B. Sporn, K.T. Liby, Nat. Clin. Pract. Oncol. 2 (2005) 518–525.
[2] N.J. Hail, M. Cortes, E.N. Drake, J.E. Spallholz, Free Rad. Biol. Med. 45 (2008) 97–110.
[3] C. Chen, A.N.T. Kong, Trends Pharmacol. Sci. 26 (2005) 318–326.
[4] Y.J. Surh, Nature Rev. Cancer 3 (2003) 768–780.
[5] B.B. Aggarwal, H. Ichikawa, Cell Cycle 4 (2005) 1201–1215.
[6] A. Scalbert, C. Manach, C. Morqand, C. Remesy, L. Jimenez, Crit. Rev. Food Sci. Nutr. 45 (2005) 287–306.
[7] S. Yannai, A.J. Day, G. Williamson, M.J.C. Rhodes, Food Chem. Toxicol. 36 (1998) 623–630.
[8] P. Nioi, J.D. Hayes, Mutation Res. 555 (2004) 149–171.
[9] A. Giudice, M. Montella, Bioessays 28 (2006) 169–181.
[10] C. Kohle, K.W. Bock, Biochem. Pharmacol. 72 (2006) 795–805.
[11] G. Asher, J. Lotem, B. Cohen, L. Sachs, Y. Shaul, Proc. Natl. Acad. Sci. USA 30 (2001) 1188–1193.
[12] M. Cuendet, C.P. Oteham, R.C. Moon, J.M. Pezzuto, J. Nat. Prod. 69 (2006) 460–463.
[13] P.W. Pare, N. Dmitrieve, T.J. Mabry, Phytochemistry 30 (1991) 1133–1135.
[14] D.S. Jang, E.J. Park, M. Hawthorne, J.S. Vigo, J.G. Graham, F. Cabieses, B. D. Santarsiero, A.D. Mesecar, H.H.S. Fong, R.G. Mehta, J.M. Pezzuto, A. D. Kinghorn, J. Nat. Prod. 66 (2003) 583–587.
[15] P. Talalay, M.J. De Long, H.J. Prochaska, Proc. Natl. Acad. Sci. USA 85 (1988) 8261–8265.
[16] H.J. Prochaska, P. Talalay, Cancer Res. 48 (1988) 4776–4782.
[17] D.W. Nebert, A.L. Roe, M.Z. Dieter, W.A. Solis, Y. Yang, T.P. Dalton, Biochem. Pharmacol. 59 (2000) 65–85.
[18] J.P. Whitlock, Annu. Rev. Pharmacol. Toxicol. 39 (1999) 103–125.
[19] F.P. Guengerich, T. Shimada, Mutat Res. 400 (1998) 201–213.
[20] P. Talalay, Chemical protection against cancer by induction of electrophile detoxication (Phase II) enzymes. in: V. Steel, G.D. Stoner, C.W. Boone, G.J. Kelloff (Eds.), Cellular and Molecular Targets for Chemoprevention. CRC Press, Boca Raton, FL, 1992, pp. 193–203.
[21] W. Li, A.N. Kong, Mol. Carcinogenesis 48 (2009) 91–104.
[22] Y.Y. Lee-Hilz, S. ter Borg, W.J.H. van Berkel, I.M.C.M. Rietjens, J.M. Aarts, Toxicol. In vitro 22 (2008) 921–926.
[23] A. Galijatovic, U.K. Walle, T. Walle, Pharmaceut. Res. 17 (2000) 21–26.
[24] B.S. Bock-Hennig, C. Kohle, K. Nill, K.W. Bock, Biochem. Pharmacol. 63 (2002) 123–128.
[25] N.J. Lawrence, D. Rennison, A.T. McGown, J.A. Hadfield, Bioorg. Med. Chem. Lett. 13 (2003) 3759–3763.
[26] S. Okombi, D. Rival, S. Bonnet, A. Mariotte, E. Perrier, A. Boumendjel, J. Med. Chem. 49 (2006) 329–333.
[27] N.C. Veitch, R.J. Grayer, Nat. Prod. Rep 25 (2008) 555–611.
[28] N.P. Craig, J. Med. Chem. 14 (1971) 680–684.
[29] C. Beney, A. Mariotte, A. Boumendjel, Heterocycles 55 (2001) 967–972.
[30] L.C. King, G.K. Ostrum, J. Org. Chem. 29 (1964) 3459–3461.
[31] J. Gripenberg, B. Juselius, Acta Chem. Scand. 8 (1954) 734–737.
[32] K. Thakkar, M. Cushman, J. Org. Chem. 60 (1995) 6499–6510.
[33] A. Ur-Rahman, M.I. Choudhary, S. Hayat, A.M. Kahn, A. Ahmed, Chem. Pharm. Bull. 49 (2001) 105–107.
[34] H.M. Sim, C.Y. Lee, P.L.R. Ee, M.L. Go, Eur. J. Pharm. Sci. 35 (2008) 293–306.
[35] S. Venkateswarlu, G.K. Panchagnula, M.B. Guraiah, G.V. Subbaraju, Tetrahedron 62 (2006) 9855–9860.

[36] A.T. Dinkova-Kostova, K.T. Liby, K.K. Stephenson, W.D. Holtzclaw, X. Gao, N. Suh, C. Williams, R. Risingsong, T. Honda, G.W. Gribble, M.B. Sporn, P. Talalay, Proc. Natl. Acad. Sci. USA 102 (2005) 4584–4589.
[37] S. Dhakshinamoorthy, A.G. Porter, J. Biol. Chem. 279 (2004) 20096–20107.
[38] A.C. Wild, R.T. Mulcahy, Free Radic. Res. 32 (2000) 281–301.
[39] Z.H. Chen, Y. Saito, Y. Yoshida, A. Sekine, N. Noguchi, E. Niki, J. Biol. Chem. 280 (2005) 41921–41927.
[40] J. Zhang, V. Svehlikova, Y. Bao, A.F. Howie, G.J. Beckett, G. Williamson, Carcinogenesis 24 (2003) 497–503.
[41] D. Livingstone, Data Analysis for Chemists. Oxford University Press, Oxford, 1995.
[42] D. Rogers, A.J. Hopfinger, J. Chem. Inf. Comput. Sci. 34 (1994) 854–866.
[43] C. Bonnesen, I.M. Eggleston, J.D. Hayes, Cancer Res. 61 (2001) 6120–6130.
[44] C. Kohle, K.W. Bock, Biochem. Pharmacol. 73 (2007) 1853–1862.
[45] W. Miao, L. Hu, P.J. Scrivens, G. Batist, J. Biol. Chem. 280 (2005) 20340–20348.
[46] Y.Y. Lee-Hilz, A.M. Boerboom, A.H. Westphal, W.J. Berkel, J.M. Aarts, I.M. Rietjens, Chem. Res. Toxicol. 19 (2006) 1499–1505.
[47] H. van der Woude, M.G. Boersma, G.M. Alink, J. Vervoort, I.M. Rietjens, Chem. Biol. Interact. 160 (2006) 193–203.
[48] V. Zoete, M. Rougee, A.T. Dinkova-Kostova, P. Talalay, R.V. Bensasson, Free Rad. Biol. Med. 36 (2004) 1418–1423.
[49] R.V. Bensasson, V. Zoete, A.T. Dinkova-Kostova, P. Talalay, Chem. Res. Toxicol. 21 (2008) 805–821.
[50] A.M. Boerboom, M. Vermeulen, H. van der Woude, B.I. Bremer, Y.Y. Lee-Hilz, E. Kampman, P.J. van Bladeren, I.M. Rietjens, J.M. Aarts, Biochem. Pharmacol. 72 (2006) 217–226.
[51] I.J. Lee, K.S. Jeong, B.J. Roberts, A.T. Kallarakal, P. Fernandez-Salguero, F.J. Gonzalez, B.J. Song, Mol. Pharmacol. 49 (1996) 980–988.
[52] M.C. Kloetzel, R.P. Dayton, B.Y. Abadir, J. Org. Chem. 20 (1955) 38–49.
[53] J.S.H. Davies, P.A. McCrea, W.L. Norris, G.R. Ramage, J. Chem. Soc. (1950) 3206–3213.
[54] J.W. Fahey, A.T. Dinkova-Kostova, K.K. Stephenson, P. Talalay, Methods Enzymol. 382 (2004) 243–258.
[55] A. Marchand, R. Barouki, M. Garlatti, Mol. Pharmacol. 65 (2004) 1029–1037.
[56] T. Mosmann, J. Immunol. Methods 65 (1983) 55.
[57] F. Tietze, Anal. Biochem. 27 (1969) 502–522.
[58] M.M. Bradford, Anal. Biochem. 72 (1976) 248–254.
[59] E.S. Arner, A. Holmgren, Measurement of thioredoxin and thioredoxin reductase. in: M.D. Maines, L.G. Costa, D.J. Reed, S. Sassa, I.G. Sipes (Eds.), Current Protocols in Toxicology. John Wiley & Sons, New York, 2000 Suppl. 5, pp. 7.4.1–7.4.14.